Anal. Chem. **2002,** *74,* 4913−4918

High-Pressure Microfluidic Control in Lab-on-a-Chip Devices Using Mobile Polymer Monoliths

Ernest F. Hasselbrink, Jr.,*,† Timothy J. Shepodd, and Jason E. Rehm‡

Sandia National Laboratories, P.O. Box 969, Livermore, California 94551

We have developed a nonstick polymer formulation for creating moving parts inside of microfluidic channels and have applied the technique to create piston-based devices that overcome several microfluidic flow control challenges. The parts were created by completely filling the channels of a glass microfluidic chip with the monomer/solvent/initiator components of a nonstick photopolymer and then selectively exposing the chip to UV light in order to define mobile pistons (or other quasi-two-dimensional shapes) inside the channels. Stops defined in the substrate prevent the part from flushing out of the device but also provide sealing surfaces so that valves and other flow control devices are possible. Sealing against pressures greater than 30 MPa (4500 psi) and actuation times less than 33 ms are observed. An on-chip check valve, a diverter valve, and a 10-nL pipet are demonstrated. This valving technology, coupled with high-pressure electrokinetic pumps, should make it possible to create a completely integrated HPLC system on a chip.

Microfluidics is just beginning to fulfill some of its promise for use in highly integrated chemical synthesis and analysis systems on the microscale.[1−3] Mathies and co-workers[4] noted that microfluidic systems have already demonstrated order of magnitude improvements in certain metrics of value, e.g., the number of separation columns that have been placed on a single wafer. In analogies between fluid motion and electricity (dating back to Benjamin Franklin and his "electric fluid" theory for Leyden jar behavior[5]), pipes are resistor analogues, valves are transistor analogues, check valves are diode analogues, and accumulators are capacitor analogues. Although this analogy is quite limited (and can be misleading), it underscores the central role of valves, check valves, and accumulators for large-scale integration.

A diversity of fluid properties and microfluidic device applications translates into a wide variety of requirements in microscale flow control. For example, a combinatorial synthesis system may require thousands of valves that operate at small or modest pressure. A multiplexed electrophoresis system may require valves that have high breakdown potentials. And a multiplexed chip-based HPLC system may require valves that seal against high pressures and are solvent-resistant. On the other hand, practical microvalves should be inexpensive to fabricate and must be compatible with substrate materials. Valves are not the only fluid-handling challenge: microscale fluid accumulators can also be a significant practical engineering challenge, since evaporation of nanoliters of material occurs quite quickly, and even a highly compliant membrane may create undesired pressure-driven flow once it is flexed.

This variety of needs has stimulated the development of a panoply of novel microflow control methods, none of which appears to be a cure-all. A large body of research using traditional MEMS materials has been directed to developing microvalves, including piezoelectric devices, silicon devices, and devices driven by shape-memory alloys;[6−11] due to materials' stiffness, these devices inevitably seem to suffer from leakage problems or dissipate relatively large amounts of power when active. For purely electroosmotic flow control, FlowFETs have been developed in Si/Si_3N_4 devices where the charge in the Debye layer is depleted by a transverse electric field.[12] Furthermore, recent work developing valves and other microfluidic devices in soft materials appears promising.[13] Pumps and valves created using multiple layers of intersecting channels in poly(dimethylsiloxane) (PDMS)[14,15] have excellent sealing characteristics and allow large-scale integration of hundreds of pressure-driven flow control devices on a single substrate; however, they are limited to pressures of about 10−20

* To whom correspondence should be addressed. E-mail: efhass@umich.edu. Phone: 734-647-7859.

† Present address: Department of Mechanical Engineering, 2250 G.G. Brown Bldg., 2350 Hayward Ave., University of Michigan, Ann Arbor, MI 48109-2125.

‡ Present address: Eksigent Technologies, 2021 Las Positas Court Suite 161, Livermore, CA 94550.

(1) Manz, A.; Graber, N.; Widmer, H. M. *Sens. Actuators, B* **1990**, *1*, 244−248.
(2) Sanders, G. H. W.; Manz, A. *Trends Anal. Chem.* **2000**, *19*, 364−378.
(3) Burns, M. A.; Johnson, B. N.; Brahmasandra, S. N.; Handique, K.; Webster, J. R.; Krishnan, M.; Sammarco, T. S.; Man, P. M.; Jones, D.; Heldsinger, D.; Mastrangelo, C. H.; Burke, D. T. *Science* **1998**, *282*, 484−487.
(4) Medintz, I. L.; Paegel, B. M.; Mathies, R. A. *J. Chromatogr., A* **2001**, *924*, 265−270.
(5) Franklin, B. *Benjamin Franklin; a biography in his own words*; Newsweek; Harper & Row: New York, 1972.
(6) Shoji, S.; Esashi, M. *J. Micromech. Microeng.* **1994**, *4*, 157−171.
(7) Bohm, S.; Burger, G. J.; Korthorst, M. T.; Roseboom, F. *Sens. Actuators, A* **2000**, *80*, 77−83.
(8) Kohl, A.; Gobes, J.; Krevet, B. *Int. J. Appl. Electromagn. Mech.* **2000**, *12*, 71−77.
(9) Emmer, A.; Jansson, M.; Roeraade, J.; Lindberg, U.; Hok, B. *J. Microcolumn Sep.* **1992**, *4*, 13−15.
(10) Esashi, M.; Shoji, S.; Nakano, A. *Sens. Actuators* **1989**, *20*, 163−169.
(11) Jerman, H. *Meas. Control* **1994**, 137−145.
(12) Schasfoort, R. B. M.; Schlautmann, S.; Hendrikse, J.; van denBerg, A. *Science* **1999**, *286*, 942−945.
(13) Whitesides, G. M.; Ostuni, E.; Takayama, S.; Jiang, X. Y.; Ingber, D. E. *Annu. Rev. Biomed. Eng.* **2001**, *3*, 335−373.
(14) Unger, M. A.; Chou, H. P.; Thorsen, T.; Scherer, A.; Quake, S. R. *Science* **2000**, *288*, 113−116.
(15) Yang, X.; Grosjean, C.; Tai, Y.-C.; Ho, C.-M. *Sens. Actuators, A* **1998**, *64*, 101−108.

10.1021/ac025761u CCC: $22.00
Published on Web 08/29/2002

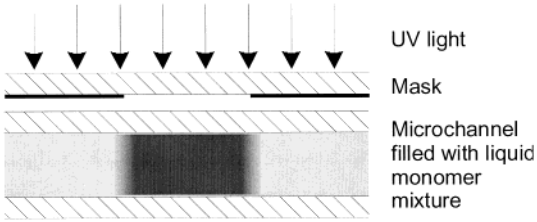

Figure 1. Method for in situ photopolymerization of mobile polymer pistons.

kPa and are incompatible with organic solvent.[15] Hydrogel valves[16] show good sealing, and their apparent weakness—the dependence of their state on fluid properties—has been largely overcome by engineering, and offer the intriguing possibility of autonomous flow control. Their actuation times are dramatically reduced at the microscale but are still on the order of a few seconds. None of these devices, however, provide low-leakage performance at pressures exceeding several atmospheres, and only a few are compatible with organic solvents.

In the present work, we create moving micropistons in situ within microfluidic channels, using laser polymerization of a nonstick polymer. Using various microfluidic channel geometries, one can create check valves, diverter valves, and pipets within the microfluidic device in a matter of a few minutes. The major advantage of this technique is that moving parts may be made without the limitations and difficulties imposed by the need for sacrificial layers or mechanical assembly, bringing at least part of the fabrication out of the cleanroom and into the chemistry laboratory. This in situ technique also allows one to fabricate moving parts that would be difficult or impossible to make using traditional buildup and etch-away techniques.

MATERIALS AND METHODS

Freely moving microparts were created by selectively photopolymerizing a Teflon-like polymer formulation inside of a microchannel.[17] As illustrated in Figure 1, the microfluidic channel is completely filled with a monomer/solvent/initiator mixture, and the mixture is then selectively exposed to UV light through a mask. Unwanted monomer is flushed away with organic solvent (via alternate conduits in the microfluidic system), while the moving part is held captive by geometric constrictions within the channel. The technique is similar to recent work on the photopolymerization of static devices (e.g., to create microfluidic platforms and stationary porous media[18,19]); in the current work, we have successfully identified formulations and polymerization methods for UV photopolymers that can move freely within microchannels. Typical formulations used in the examples presented here are as follows: (monomers) 1:1 trifluoroethyl acrylate/1,3-butanediol diacrylate (50−80%); (solvents) methoxyethanol/1,4-dioxane/5 mM TRIS buffer (total 20−50%); and (photoinitiator) 2,2′-azobisisobutyronitrile 0.5% (w/w). Polymerization and cross-linking is initiated by 355-nm light from a Nd:YAG laser (1

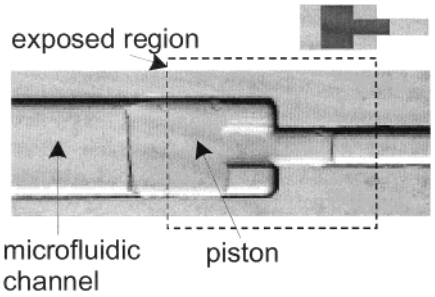

Figure 2. Photopolymerized piston with cross-sectional area change. The width of the channel contracts from 150 to 50 μm, and the channel is 25 μm deep. The piston was UV-polymerized in the outlined region and then displaced slightly to the left to show the molded sealing surface. Plastic deformation of the piston is not observed until the pressure applied at left exceeds 300 bar.

(mJ cm^{-2})/pulse, 10 Hz) through a chrome-on-quartz mask for 30−75 s. Although a number of UV sources will initiate photopolymerization, a laser confers higher resolution photodefinition of the part. All reagents are used as received from Sigma-Aldrich, except the monomers, which are purified with activated white quartz sand just prior to use.

Resolution of the devices is limited by the competition between radical diffusion and initiation/recombination reactions. Typical resolution achieved is ~10 μm, achieved by allowing oxygen to diffuse into the formula prior to polymerization.

Figure 2 shows an illustrative example of a piston created in a microfluidic channel (in a glass chip) that has a reduction of its cross-sectional area (see inset). The monomer solution was exposed to UV in the rectangular region outlined by the dashed line and has been moved to the left by applying pressure at the right inlet (using finger pressure applied to a syringe, which is coupled to the chip via silica capillary and custom-made glue-down ferruled fittings similar to ones now sold commercially by Upchurch, Inc., Oak Harbor, WA). The piston is difficult to see due to its optical clarity; the drawing above the image is intended to guide the reader's eye to the outline of the piston.

DEVICE EXAMPLES AND PERFORMANCE

One important point illustrated by Figure 2 is that because the part is automatically molded to the cross-sectional shape of the microchannel, and because it is polymerized against the channel constriction, tight sealing is automatically achieved, as will be demonstrated shortly. This makes this technique particularly well-suited to fluid control applications in microdevices; in fact, we have found in work conducted thus far that liquid is necessary as a lubricant.

Simple geometries of channel and piston lead to a wide variety of devices, wherein the channel constrictions behave as stops or as sealing surfaces for pistons. In Figure 3, a check valve only allows unidirectional flow, due to the location of the piston relative to a bypass channel. Figure 3a shows a three-dimensional schematic of both the substrate (clear) and the piston (gray). Cylindrical channels were constructed by wet-etching mirror images of the channel geometry in two glass wafers and then bonding them together using electrostatic bonding followed by thermal annealing. Two depths of channel were created, by etching each wafer twice (first etching just the deep channels and then repeating the photoresist/expose/develop/etch process for

(16) Beebe, D. J.; Moore, J. S.; Bauer, J. M.; Yu, Q.; Liu, R. H.; Devadoss, C.; Jo, B. H. *Nature* **2000**, *404*, 588.
(17) Rehm, J. E.; Shepodd, T. J.; Hasselbrink, E. F.; Kluwer Academic: Monterey, CA, 2001; pp 227−229.
(18) Svec, F.; J., F. J. M. *Science* **1996**, *273*, 205−211.
(19) Beebe, D. J.; Moore, J. S.; Yu, Q.; Liu, R. H.; Kraft, M. L.; Jo, B. H.; Devadoss, C. *Proc. Natl. Acad. Sci. U.S.A.* **2000**, *97*, 13488−13493.

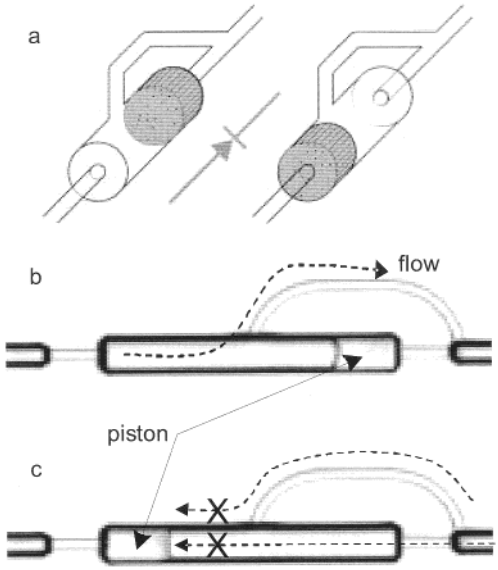

Figure 3. On-chip passive check valve. (a) Schematic of valve architecture. The concentric cylinder (with bypass) geometry is created in the substrate (shown clear) by wet-etching mirror images of half-cylinders in two substrates, then aligning, and bonding. The free piston (gray) is polymerized in situ. Both glass wafer surfaces are HF-etched (in mirror image) to produce interconnecting channels of concentric cylinders when bonded. (b) Flow direction is indicated by dashed lines. Flow from left to right bypasses the piston seated against the right stop. (c) Flow from right to left is prevented when the piston seats against the left stop, checking the flow. Cylinder diameters are approximately 100 and 25 μm.

the shallower features). Although hemispherical channels (with only one side etched) are significantly easier to fabricate, they allow more leakage to occur, for lack of a sealing surface around the entire circumference of the end of the piston. Sections b and c of Figure 3 show the check valve (a "diode", pointing to the right) in operation. In Figure 3b, the piston allows flow past the piston via a bypass channel, while the piston is seated against the stop at right. In Figure 3c, the piston is seated against the left stop, preventing any flow from passing through. An important engineering tradeoff in the design of these systems is, of course, the amount of leakage that occurs through the bypass while the piston is actuated from left to right. Assuming Poiseuille flow in the bypass, the volume of fluid that leaks past the piston during actuation is $Q_{leak} \approx (\pi d_b^4/128\eta L_b)\Delta P_{act}\Delta t_{act}$, where d_b and L_b are the bypass channel hydraulic diameter and length, respectively. Since the leakage will be proportional to the product of the pressure differential across the piston ΔP_{act} and the time required for it to actuate Δt_{act}, clearly a low-friction piston leads to lower leakage. For a piston/channel of fixed friction characteristics, the engineering tradeoff that must be considered in selecting the design variables d_b and L_b is the amount of pressure drop that is tolerable during forward-flow operation (similar design compromises are encountered with macroscale check valves). Since the leakage scales with the fourth power of d_b, this is a very influential design variable.

Figure 4 shows a diverter valve (analogous to an exclusive OR gate), created by polymerizing a piston between two stops that surround the intersection of two channels. The valve allows the injection of fluid into a device from either input, while largely restricting unwanted flow into, and contamination of, the opposite

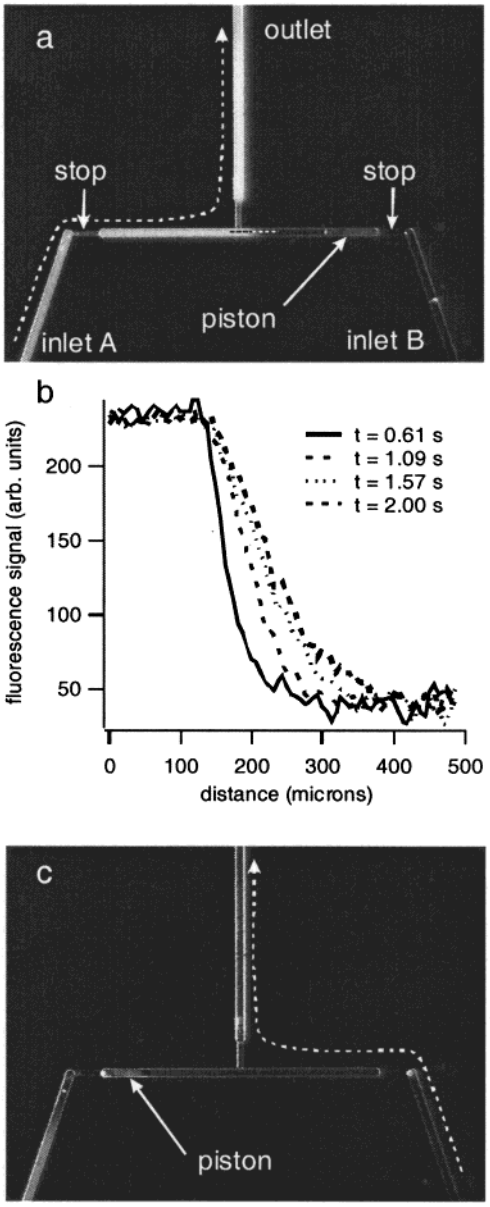

Figure 4. Diverter valve. Large channels are ~75 μm in diameter, with 25-μm-diameter constrictions at the piston seats. (a) Pressure (~1 MPa) is applied to fluorescent dye solution at inlet A; the piston seats to the right, preventing cross-contamination of inlet B while dye solution flows into the device. (b) Profiles of the dye signal profiles through the dashed line, as a function of time. Exponential curve fits indicate the front is moving ~115 μm in 1.6 s; diffusion alone over this time would give a front moving 56 μm, assuming $D = 10^{-9}$ m^2/s. This suggests leakage at a velocity of ~37 μm/s or a leakage flow rate of ~160 pL/s for this channel diameter of 75 μm. (c) Pressure is applied from inlet B, at right, and the piston seats against the left stop. Some leakage is apparent (notice the low dye signal in inlet A) due to imperfect matching of the piston to the stop.

input. The channels are created in a manner similar to those in Figure 3, with stops as shown in Figure 4a. In Figure 4a, fluorescent dye solution is being injected at ~2 MPa (300 psi) pressure into the chip; based on calculated Darcy restrictions from inlet to outlet, the pressure differential across the polymer plug is ~1 MPa.

Leakage past the piston was quantified in this diverter valve, by digitizing the video of the fluorescence interface near the

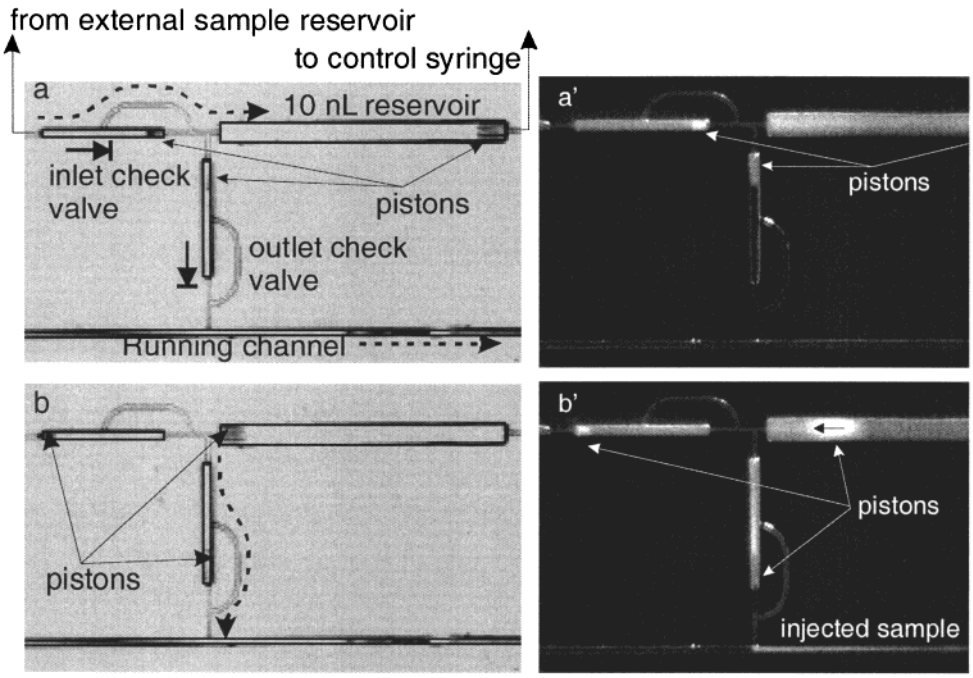

Figure 5. A 10-nL pipet. Check valves (as in Figure 3) are placed at sample inlet and pipet outlet, and a simple piston/cylinder reservoir is placed between the sample inlet and a control inlet. The outlet of the pipet issues into a pressurized channel at the bottom of the images, flowing from left to right. Dashed lines indicate sample flow. The left images are broadband illumination images of the pistons; the right images are fluorescence images; only the sample contains dye. Top (a, a′): Suction is applied at the control reservoir; in response, the piston in the reservoir moves to the right, drawing sample through the open check valve, until the reservoir at inlet B is filled. The check valve at the pipet outlet remains closed. Bottom (b, b′): Pressure is applied at inlet B; the check valve at inlet A closes, the valve at outlet C opens, and the fluid in cylinder B is injected into the channel.

intersection and then extracting these profiles as shown in Figure 4b. After accounting for interface broadening due to molecular diffusion, the profiles show a leakage rate of ~160 pL/s (see caption for details). For comparison, without the piston, the flow rate through inlet B is ~20 μL/s (as calculated by assuming Poiseuille flow through a capillary of this diameter and length).

The leakage rate, however, depends on the details of the polymerization method. We note that the leakage is noticeably greater when the piston is seated against the left stop (~1 nL/s), as evidenced by the receding dye fluorescence in Figure 4c. This asymmetric sealing behavior is not by chance. In this particular case, the piston was polymerized at the right stop (near inlet B), and so it automatically assumes a conforming shape; however, the left end of the piston was defined only by the mask, and so it does not conform exactly to the (isotropically etched) shape of the left stop. Therefore, the leakage is naturally higher on the left side, because the sealing surfaces are not perfectly matched. For applications where bidirectional sealing is needed, a two-step polymerization process (e.g., polymerize against the right stop, move the piston to the left stop, and then continue polymerizing with a second mask) may be necessary; we will be addressing this issue in future work.

More complex functions can be performed with combinations of these simple elements. For example, in Figure 5, a 10-nL pipet (composed of a piston/cylinder reservoir, combined with two check valves) is demonstrated. Optical images are shown at left, and fluorescence images at right, as a sample is delivered from a sample reservoir to a pressurized channel of fluid running from left to right at the bottom of Figure 5. The "reservoir" formed by the piston/cylinder, at the upper right, is connected to an inlet/outlet port on the chip, to which a syringe is connected via capillary tubing. Manually drawing vacuum on the syringe draws the piston to the right until it reaches the stop (Figure 5a,a′); during this "draw" step, fluid is drawn primarily from the sample reservoir through the inlet check valve because the outlet check valve closes. Manually applying pressure on the syringe pushes the reservoir piston to the left until it reaches the left stop (Figure 5b,b′); during this "dispense" step, the fluid flows out through the outlet check valve because the inlet check valve closes. Device performance is not perfect, however; minor leakage is apparent. Reasons for the leakage include polymerizing the pistons against only one of the stops and leakage past the check valve during the time it takes for it to close, as discussed previously.

Maximum pressure, actuation speed, and leakage tests were performed in silica capillaries and glass chips in a configuration similar to that shown in Figure 3. In the highest pressure cases (where maximum pressures for certain formulations exceeded the 3000 psi limits of our glass chips and fittings), pistons were polymerized in 100-μm-i.d. silica capillary, butted against a 50-μm capillary using a zero dead-volume connecter. Pressure was gradually increased with an HPLC pump, and the junctions were observed under the microscope for leakage (evidenced by bubbles introduced into the channels) or plastic deformation of the pistons. Maximum pressures observed were 34 MPa (5000 psi). Actuation times are less than 1 video frame (33 ms), as observed by digitizing video frames such as those in Figure 4. Actuation pressure can be less than 7 kPa (1 psi), as will be demonstrated shortly in Figure 7. Leakage around these pistons is difficult to measure; however, it was found that much lower leakage rates resulted when plugs were polymerized in place against their stops.

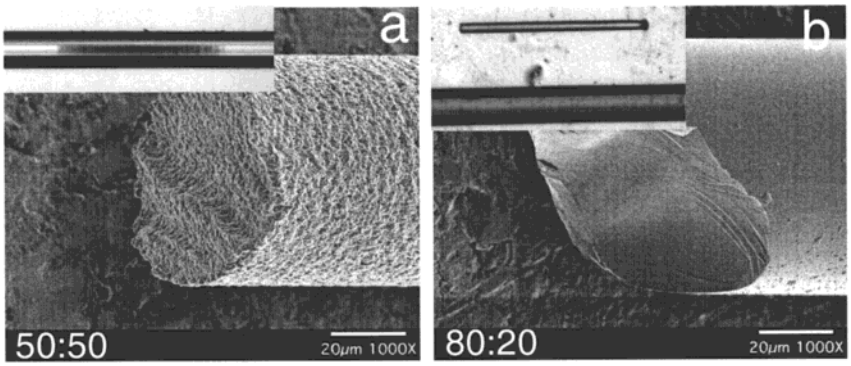

Figure 6. Porous and non- (or nano-)porous pistons. (a) Scanning electron micrograph (SEM) of a porous piston. Note that the rough edge of the piston is due to fracturing the piston after ejecting it from the capillary. Inset image is an optical image of a similar piston just after photopolymerization in a 75-μm-diameter capillary. (b) SEM of a 75-μm-diameter non- (or nano-)porous piston, shown after ejecting it from its capillary (inset).

Perhaps not surprisingly, it was observed that the leakage rate is not monotonic with pressure;[10] for example, one class of polymers had maximum leakage rates at 0.4−0.8 MPa (depending on the degree of cross-linking), which improved dramatically as pressure increased to 10 MPa. The improvement in sealing with higher pressures appears to result from better conformation of the soft polymer to the glass substrate.

PISTON PROPERTIES

A wide range of polymer properties is possible by varying formulation and polymerization procedures. Work on microporous polymer materials for capillary electrochromatography[21−23] has shown that varying the solvent/monomer ratio in a phase-change polymerization strongly affects the pore size and porosity. It has also been shown that small amounts of additives such as 0.5% (2-(acryloyloxy)ethyl)trimethylammonium methyl sulfate and 2-acrylamido-2-methyl-1-propanesulfonic acid (AMPS) create surface terminal groups that are charged at neutral pH, so that the polymer monoliths support electroosmotic flow. Thus charged monoliths can either move freely as macro-ions or, when porous, can support electroosmotic flow through themselves when their own motion is constrained. And of course, the degree of polymerization and cross-linking directly affects the mechanical strength of the polymer. The critical parameters determining the behavior of these parts in microfluidic control applications are the porosity, mean pore size, elastic modulus, and friction coefficient with the wall.

Figure 6 illustrates the variable porosity of the piston that can be achieved simply by changing the monomer/solvent ratio of the formulation. Figure 6a shows the first mobile piston we produced, polymerized in a 75-μm-diameter capillary. It is porous; the formulation used (50% monomer (70:30 butyl acrylate/1,3 butanediol diacrylate)) undergoes phase separation during polymerization. Figure 6b shows a nonporous (or nanoporous) piston (80% monomer) that has been ejected from the capillary; this piston was created from a fluorinated monomer formulation used for most of the devices illustrated in this work. Smaller pores in this piston result from phase change occurring much later in the polymerization process.

By polymerizing a piston upstream of a constriction in the channel, and applying high pressure, the compression of the piston gives an order of magnitude estimate of its compressive strength. Tests conducted in this way indicate that, depending on the degree of polymerization, elements have a modulus of elasticity similar to a common rubber stopper (0.01−0.1 GN/m^2). This method relies on some shrinkage of the polymer within the channel to prevent overconstraining the mechanical system or the assumption that the material possesses a very low Poisson's ratio. Furthermore, the modulus is strongly dependent on the degree of polymerization, which depends strongly on the dose of UV exposure. For example, we have made very soft, almost gelatinous pistons that are flexible enough to negotiate 50-μm radius, 90-deg bends in 50-μm-wide channels with ease and pistons that can easily squeeze into channels that are ∼30% smaller than their (unconstrained) width. However, these are only weakly cross-linked and have fairly low mechanical strength.

Static friction is another critical parameter governing the utility of these devices. Tests were performed to determine the static friction coefficient by slowly increasing the pressure applied across simple pistons polymerized in a commercial silica capillary (similar to those in Figure 6, using a non- or nanoporous polymer), until the piston began to move. The axial force on the piston is the product of the applied pressure and cross-sectional area of the piston A_x; the contact surface area between the capillary and piston, A_s, is determined by the diameter and length of the piston. We hypothesize that the static friction is generated either by a density of chemical bonds between the polymer and the glass or by normal force created by osmotic pressure in the piston (observed as swelling of the polymer when it is unconstrained). In either case, the normal force is proportional to A_s, and taking n_s as the coefficient of static friction, we expect $P_s A_x \sim A_s n_s$, where P_s is the pressure required to move the piston. We also expect that n_s is only a function of polymer formulation and the degree of polymerization. These expectations were investigated by polymerizing plugs of 1-mm length using a range of UV exposures and in three different diameters of capillary (25, 50, and 75 μm).

(20) Paul, P. H.; Arnold, D. W.; Rakestraw, D. J. Kluwer Academic: London, 1998; pp 49−52.
(21) Ngola, S. M.; Fintschenko, Y.; Choi, W. Y.; Shepodd, T. J. *Anal. Chem.* **2001**, *73*, 849−856.
(22) Lammerhofer, M.; Svec, F.; Frechet, J. M. J.; Lindner, W. *J. Chromatogr.* **2001**, *925*, 265−277.
(23) Viklund, C.; Nordstrom, A.; Irgum, K.; Svec, F.; Frechet, J. M. J. *Macromolecules* **2001**, *34*, 4361−4369.

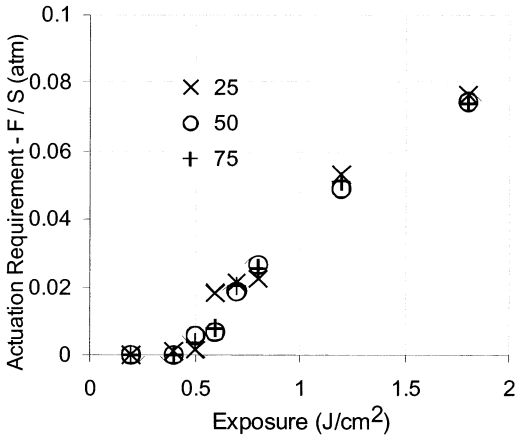

Figure 7. Actuation force required to mobilize pistons. Normalizing the force, *F* (pressure differential × channel cross-sectional area), by the surface area in contact with the channel, S, collapses the data to a single curve.

Figure 7 shows data for a particular polymer formulation, plotted as $P_s A_x / A_s$ versus exposure. The data collapse to a single curve, which at least verifies the scaling equation and the dependency of n_s on exposure dose. Repeatability of these data was not tested, but the fact that the scatter is relatively low, and that each data point represents a different piston, suggests that for a given polymer formulation this behavior is quite deterministic. The test is inconclusive, however, as to the cause of the static friction force. Tests on macroscale pistons created in 2-mL vials are similarly inconclusive, as the fluorinated polymers in these vials do not appear to stick at all. Furthermore, it has been noticed that stiction coefficients are higher in etched channels than in silica capillary, suggesting that nanoscale roughness in the etched channels may be a factor.

Last but not least, it is important to note that the material formulations presented here perform best in relatively high concentrations of organic solvent. Depending on monomer mixture formulation, significant shrinking in water (as little as 3% and as much as 35%) has been observed. Recent work in our laboratory has focused on this issue and identified nonstick photopolymers with minimal shrinkage/swelling.[24]

CONCLUSIONS AND FUTURE WORK

One can create moving micropistons in situ within microfluidic channels, using laser polymerization of a "nonstick" polymer. Using various microfluidic channel geometries, one can create check valves, diverter valves, and pipets within the microfluidic device in a matter of a few minutes. The major advantage of this technique is that moving parts may be made without the limitations and difficulties imposed by the need for sacrificial layers or mechanical assembly. Furthermore, the use of a "soft" piston material leads to excellent sealing characteristics (<200 pL/s) and the devices can withstand very high pressures (>30 MPa). These devices do require that a conduit for flushing out unwanted monomer is available after photopolymerization. For some devices, this may mean that vestigial channels and ports may remain after device fabrication is complete.

Significant work remains to be done before commercial deployment of a microfluidic control system based on this technology is possible. Detailed characterization of polymer characteristics (especially leaching) and several improvements remain to be done. For example, the material formulations presented here may be subject to shrinking and swelling as discussed in the previous section. Improving bidirectional sealing of the pistons (reducing the asymmetry of the sealing with a two-step polymerization process) also remains to be done.

We note that the application of these devices is not necessarily limited to microfluidics. Nonstick photopolymers make it possible to fabricate moving parts, which would be difficult or impossible using traditional etching techniques, and the compatibility of these devices with water avoids stiction problems often encountered in silicon-based MEMS devices. Of course, many MEMS applications require that they avoid liquid immersion for other reasons (e.g., high-frequency response).

(24) Kirby, B. K.; Shepodd, T. J.; Hasselbrink, E. F. *J. Chromatogr., A*, submitted.

ACKNOWLEDGMENT

This work was supported by the LDRD program at Sandia National Laboratories. Sandia is operated for the United States Department of Energy under Contract DE-AC04-94AL85000. The authors acknowledge the technical assistance of Dr. Sarah Ngola, Mr. Ken Hencken, and Mr. George Sartor. High-pressure fittings for chip-to-capillary connections, designed and fabricated by Mr. Ron Renzi, were critical to the completion of this work.

Received for review May 10, 2002. Accepted July 20, 2002.

AC025761U